Analysis of residual stress relaxation under mechanical cyclic loading of shot-peened trip780 steel until fatigue lifetime

Clément Mauduit [a,b], Régis Kubler [b], Laurent Barrallier [b], Sophie Berveiller [c], Quentin Puydt [a], Martine Monin [d], Bastien Weber [e]

[a] Institut de Recherche Technologique M2P, France, clement.mauduit@irt-m2p.fr, quentin.puydt@irt-m2p.fr;
[b] Arts et Métiers ParisTech, MSMP, France, regis.kubler@ensam.eu, laurent.barrallier@ensam.fr;
[c] Arts et Métiers ParisTech, LEM3, France, sophie.berveiller@ensam.eu;
[d] PSA, France, martine.monin@mpsa.com; [e] ArcelorMittal Research, France, bastien.weber@arcelormittal.com

Keywords: TRIP steel, shot-peening, residual stresses, relaxation, fatigue

Introduction and objectives

TRIP aided steels are used in the automotive industry due to their high strength, ductility and toughness properties. Typical parts made of TRIP steels (as engine sub-frame for instance) are submitted to cyclic loading during their lifetime. Those parts could be also shot-peened to minimise the risk of fatigue failure. Studies have investigated the fatigue life of non-treated TRIP aided steels [1-3], the shot peening of TRIP steels [4-9] but very few [10] have investigated the mechanical residual stress stability after shot peening on TRIP steels and the impact on fatigue life. TRIP steels exhibit a multiphased microstructure of ferrite, bainite, residual austenite and martensite created after thermomechanical loading/straining. Shot peening on TRIP steel generates austenite to martensite phase transformation and a gradient of microstructure and residual stresses from the surface as characterized by Guiheux [9].

The aim of this study is to analyse the evolution of residual stresses (RS) generated by shot-peening during cycling and the effects of shot peening on fatigue life of a cold rolled TRIP780 steel. The stability of RS was assessed using X-ray diffraction techniques. Macroscopic finite element simulation of fatigue life.

Methodology

Material and sample geometries

TRIP780 steel specimens cut from cold rolled sheets (thickness 2 mm) provided by ArcelorMittal were studied. The phase distribution of TRIP780 steel consists of about 70 % ferrite (BCC), 15 % residual austenite (FCC) and 15 % bainite. TRIP780 steel has a fine microstructure with retained austenite having an average grain size of 3 µm. Its yield stress is 560 MPa. Samples were shot-peened in a wheelblast Wheelabrator shot peening machine successively on each face. The investigated shot peening conditions for fatigue were 400 µm spherical steel shots 700 HV, coverage rate 230 %, Almen intensity: F19.1A (SP1), F9.8A (SP2).

Interrupted cyclic and fatigue bending tests were performed on specimens taken in the transverse direction of the steel sheet. As-Received (AR) and Shot-Peened (SP) specimens were investigated. Filets with a radius of 1 mm were machined at the corners of the rectangular cross section of shot peened samples in order to minimize any stress concentration effects. Only stress relaxation after SP1 condition is presented in this paper.

Plane bending cyclic and fatigue tests

A specific plane bending device developed for the CONDOR project at IRT-M2P was used for interrupted cyclic and fatigue testing. The system ran on a MTS 15 kN fatigue machine (Figure 1.a). Two samples are tested in parallel with a controlled displacement of the actuator ensuring an imposed curvature. The load and the displacement of the actuator are measured versus time. Loading ratio R = −1 is considered in this paper.

Fatigue tests were performed up to failure (N_f cycles), that corresponds to a load drop of 5% from the stabilized value. In order to study stress relaxation, some SP specimens were tested at a given

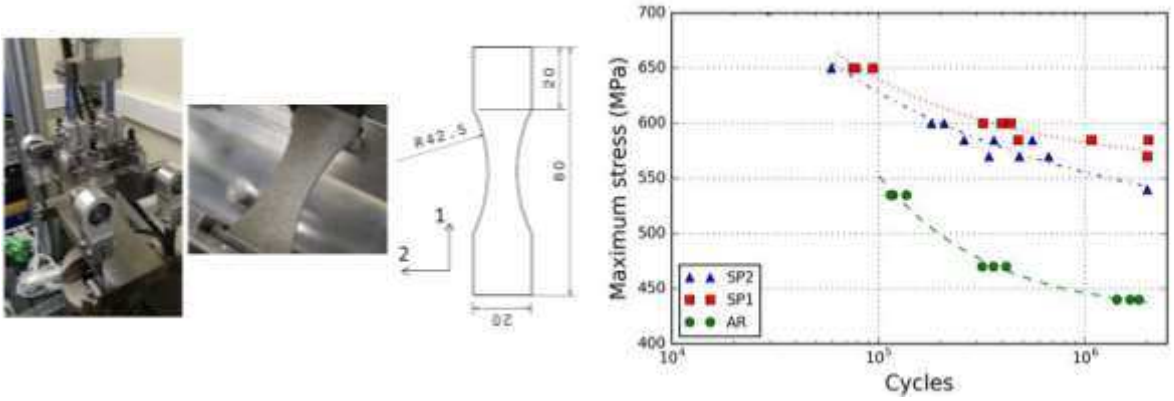

Figure 1: (a) Pure bending test device with specimen geometry. (b) Fatigue test results for R=-1.

Table 1: Stromeyer fitting parameter for Wöhler curves.

	E (MPa)	A	γ
AR	426	1,433,830	0.81
SP1	559	40,123	0.54
SP2	496	7,253	0.35

number of cycles (1000, $N_f/2$). At the failure state, specimens remained in one part exhibiting a crack at the surface. Wöhler's curves are presented in Figure 1.b. A Stromeyer fit, $\sigma = E + \frac{A}{N^{\gamma}}$, is applied with parameters E, A and γ provided in Table 1. It is observed that the applied shot peening conditions increases fatigue life of TRIP780 steel. SP1 condition gives a better fatigue life than SP2. The fatigue tests data were used to calibrate a Crossland high cycle fatigue criteria [13] for AR material.

X-ray diffraction analysis

X-ray diffraction (XRD) analysis has the ability to distinguish the constituents according to their crystallographic structure. Diffraction peaks of α′ martensite appear at the same 2θ positions as peaks of α ferrite. However, no peak separation process has been done and only the global ferritic α + α′ is considered. XRD analysis was performed to quantify the volume fraction of residual austenite f^{γ} in the depth of the specimen by analysing {110}, {200} peaks in ferritic constituents α (ferrite and martensite) and {111}, {200} peaks in austenite γ on a Siemens D500 device using a Cr radiation (V filter). ASTM 975-03 [15] standards was applied for phase determination. Residual austenite volume fraction f^{γ} was only determined if its value was more than 5%. The technique was also used to determine the stress in the longitudinal (direction 1) and in the transverse (direction 2) directions of the fatigue specimens (see Figure 1.a). The peak broadening versus number of cycles was also analyzed using the integral breadth B. XRD stress determination σ^{γ} was performed in the austenitic phase on the {311} peaks using a Mn radiation (Cr filter) with a Elphyse Set-X device. The stress in the ferritic phases σ^{α} was determined on the {211} peaks using a Cr radiation (V filter) with a Siemens D500 apparatus. 13 ψ angles were used and the $\sin^2\Psi$ method is applied as specified in [16]. For multiphased materials, $\sigma_{11} - \sigma_{33}$ is determined in each phase.

Ferritic and austenitic phases can be considered as isotropic polycrystalline materials [9]. Thus, the radiocrystallographic elastic constants are defined for each phase:

$S_1^\alpha = -1.272 \times 10^{-6}\, MPa^{-1}$, $\frac{1}{2}S_2^\alpha = 5.832 \times 10^{-6}\, MPa^{-1}$, $S_1^\gamma = -1.470 \times 10^{-6}\, MPa^{-1}$, $\frac{1}{2}S_2^\gamma = 6.410 \times 10^{-6} MPa^{-1}$.

XRD analyses were performed in the center of the specimens after electropolishing (circle of radius 3 mm) with a 1 mm diameter collimator. The determined stress was corrected in order to take into account the material removal following the modified Moore-Evans methodology proposed by Castex [11]. A mixture law is used to calculate the macroscopic RS in each direction:

$$\Sigma = f^\gamma \sigma^\gamma + (1 - f^\gamma)\sigma^\alpha \qquad (1)$$

Fatigue analysis and simulation

Observations on the specimens used to obtain the Wöhler curves were done using optical and scanning electron microscopy at the surface and at the fracture surfaces after static opening of cracks. Finite Element Analyses (FEA) were carried out to investigate the fatigue life of specimens after shot peening. Macroscopic RS were introduced using a fictitious thermal method [12]. The material behaviour is considered isotropic elastic with E = 210 GPa and ν = 0.3. For different applied cycles, a post-treatment was performed using a Crossland [13] fatigue criterion identified on experimental data.

Results and analysis

RS profile and martensitic volume fraction evolution during cyclic mechanical testing

The proportion of ferritic phases (α + α′) is close to 100% at the surface of the specimen and 87 % in the core after shot peening. No significant evolution of volume fraction of martensite was observed on a depth of 300 µm after cycling. Profiles of macroscopic RS after SP1 and bending cycles (R = -1) are presented for 600 MPa in Figure 2. Zero (0) cycle curves correspond to the initial profile of RS after shot-peening. The relaxation of RS happens in both directions. The relaxation is more important in longitudinal direction 1 than in the transverse direction 2. It is important to notice that the relaxation is also more present in the depth than at the surface of the specimen. Integral breath (B) profiles in α phase are provided in Figure 3. The peak broadening has two main contributions due to diffracting domain size and lattice distortion due to dislocations. For SP specimens, the B-profile decreases vs the depth due to inelastic strain (plasticity and phase transformation) that affects the surface during the shot peening process. This B-profile decreases vs the number of cycles showing that there is a possible dislocation rearrangement into energetically preferable positions during cycling [14]. This effect is more effective in the depth than at the surface. It can be assumed that at the surface of the specimen the dislocations structure is more stable though the stress is higher. In the present case, the shot peened state is a biaxial stress state ($\Sigma_{11} = \Sigma_{22}, \Sigma_{33} = 0$) that evolves during cycles to a bending load that acts mainly on Σ_{11}leading to an uniaxial stress state.

Fatigue analysis and simulation

The fatigue fracture surfaces were analysed after static crack opening with caution to not alter surface cracks. Figure 4 shows the fracture for the specimen loaded at 600 MPa (R = -1) until failure detection. Though the fatigue cracks occur from both surfaces, it is not always symmetric. Multiple initiation points are observed at the surface of the specimen. The surface roughness seems to play a prevalent role on the crack initiation compared to RS.

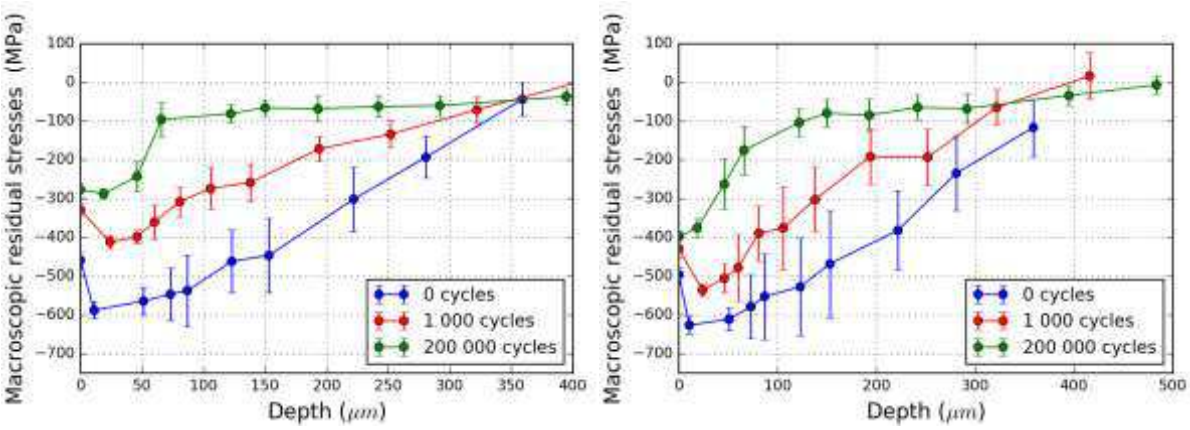

Figure 2: Macroscopic RS profiles for SP1 specimens at 600 MPa (R=-1) before cycling and after 1000 and 2.10^5 cycles. Left: Direction 1 – Right : Direction 2

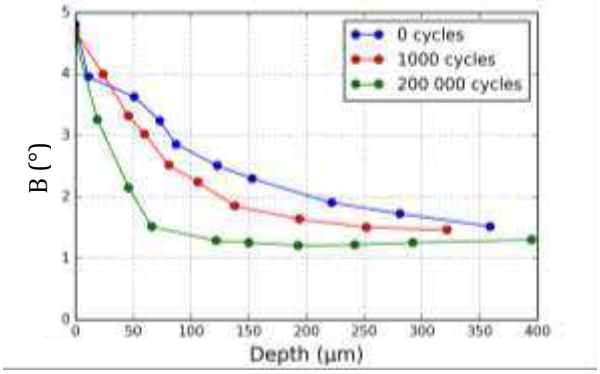

Figure 3: Integral breath profiles in α phases for SP1 specimens at 600 MPa (R=-1) before cycling and after 1000 and 2.10^5 cycles.

Figure 4: Fatigue fracture surface of the specimen loaded at 600 MPa (R=-1). (a) Global fracture surface showing the fatigue surface, (b) initiation zone identified at the surface of the specimen.

The macroscopic RS profiles at $N_f/2$ (after relaxation) were used and introduced in the depth of the specimen modeled in Abaqus (Figure 5.a). A symmetric cycle is applied to obtain the maximum stress at the surface. The superposition of the RS field with the elastic load for bending is post-treated using the Crossland criterion. A maximal limit to 10^7 cycles was set. Figure 5.b shows the predicted life time vs. depth. The minimal predicted lifetime is in good agreement with the experimental one. However, the predicted initiation point is at a depth of 100 µm whereas no initiation has been experimentally observed except on the surface. This could be explained by the

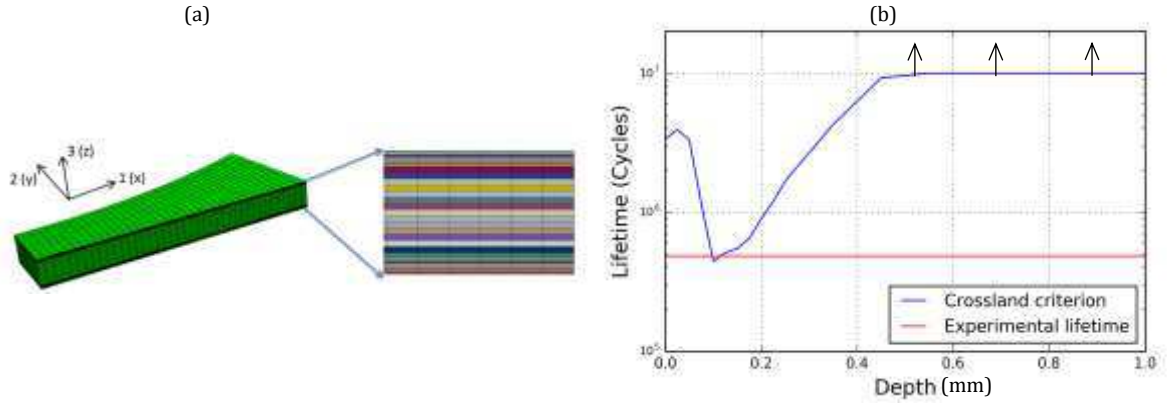

Figure 5: Fatigue simulations after shot peening. (a) Mesh discretization to introduced the residual stress profiles for SP1 conditions at $N_f/2$ (b) Fatigue life time prediction at 600 MPa (R=-1) vs the depth of the specimen (1 mm = mid-thickness) using Crossland criterion compared to experimental data.

fact that the fatigue criterion does not take into account the roughness of the surface that induces local stress concentrations. Another assumption can be the damage of the layers affected by work hardening during cycling. Some additional work will be carried on.

Conclusions

Shot peening of TRIP780 steel specimens increases their fatigue life under bending loading in the high cycle fatigue regime. Relaxation of the RS after shot-peening of a TRIP780 steel has been shown after mechanical cycling. RS do not completely disappear after half fatigue life ($N_f/2$).
By analysing the integral breath profile, the surface of the specimen is shown to be more stable than the layers in depth of the material.
FEA simulations of an elastic load superposed to RS give a good prediction of the fatigue life though the initiation point is predicted at a depth of 100 µm.
As a perspective, relaxation in the first cycles with plastic cyclic behaviour should be investigated.
For a better prediction of the fatigue initiation zone, surface roughness has to be taken into account.

Acknowledgments

We wish to thank all the partners of CONDOR project lead by IRT-M2P for their cooperation.

References

[1] R. Munier, C. Doudard, S. Calloch, B. Weber, Int. J. of Fatigue, 63 (2014) 46-61.
[2] P.I. Christodoulou, A.T. Kermanidis, D. Krizan, Int. J. of Fatigue, 91-1 (2014) 220-231.
[3] S. Ackermann, D. Kulawinski, S. Henkel, H. Biermann, Int. J. of Fatigue, 67 (2014) 123-133.
[4] G. Fargas, J. J. Roa, A. Mateo, Mater. Sci. Eng. A 641 (2015) 290–296
[5] X. Kléber and S. P. Barroso, Mater. Sci. Eng. A 527(21-22) (2010) 6046–6052.
[6] M. Turski, S. Clitheroe, AD Evans, C. Rodopoulos, Appl. Phys. A 99 (3) (2010) 549-556.
[7] P. Fu, K. Zhan, and C. Jiang, Mater. Des. 51 (2013) 309–314
[8] M. Halilovič, S. Issa, M. Wallin, H. Hallberg, and M. Ristinmaa, Int. J. Mech. Sci. 111–112 (2016) 24–34.
[9] R. Guiheux, « Comportement d'aciers à transformation de phase austénite-martensite pour la simulation du grenaillage de précontrainte ». Ph.D. Thesis, ENSAM (2016). www.theses.fr/2016ENAM0055
[10] K. Sugimoto, Y. Mizuno, M. Natori, T. Hojo, Int. J. of Fatigue, 100 (2017) 206-214.
[11] L Castex. « Redistribution des contraintes dans une plaque après enlèvement de matière ». Groupement Français pour l'analyse des contraintes par diffractométrie X (1984).
[12] M. Desvignes, Ph.D. Thesis, ENSAM (1987).
[13] B. Crossland, Proceedings of the international conference on the fatigue of metals, London (1956), 138-149.

[14] V. Schulze, Modern mechanical surface treatment – States, stability, effects. Wiley-Vch, (2003).
[15] ASTM 975-03, Standard Practice for X-Ray Determination of Retained Austenite in Steel with Near Random Crystallographic Orientation, ASTM International, West Conshohocken, PA, 2003, www.astm.org
[16] NF EN 15305, Essais non-destructifs - Méthode d'essai pour l'analyse des contraintes résiduelles par diffraction des rayons X, 2009, www.afnor.org